Measurement of Dispersive Properties of Electromagnetically Induced Transparency in Rubidium Atoms

Min Xiao, Yong-qing Li, Shao-zheng Jin, and Julio Gea-Banacloche
Department of Physics, University of Arkansas, Fayetteville, Arkansas 72701
(Received 7 March 1994; revised manuscript received 1 June 1994)

The dispersive properties of the atomic transition in the rubidium D_2 line ($5S_{1/2}-5P_{3/2}$) at 780.0 nm are measured with a Mach-Zehnder interferometer when an additional coupling field at 775.8 nm is applied to an upper transition ($5P_{3/2}-5D_{5/2}$). This ladder-type system is observed to exhibit electromagnetically induced transparency together with a rapidly varying refractive index. A reduction in group velocity for the probe beam ($v_g = c/13.2$) is inferred from the measured dispersion curve with 52.5% suppressed absorption on resonance.

PACS numbers: 42.50.Hz, 32.70.–n, 42.25.Bs, 42.65.An

Electromagnetically induced transparency (EIT) is a modification of the absorption profile of an atomic transition when the upper level is coupled coherently to a third level by a strong laser field. Under the right circumstances, the absorption of a weak probe beam at the resonance frequency can then be substantially reduced. There exists by now a large amount of literature on this subject [1–5]. A number of experiments have also been carried out [2]. In addition to the possible applications of the reduced absorption effect [3] (including lasing without inversion), the dispersion properties of these systems have also been predicted to be of interest: Harris, Field, and Kasapi have predicted a reduction in the group velocity of a pulsed probe beam [4] due to the rapidly varying refractive index near line center. Scully and Fleischhauer have considered the possibility of using the enhanced index of refraction without absorption in a novel atomic magnetometer [6].

We report here the direct measurement of the dispersive properties of an EIT medium [a gas of rubidium (Rb) atoms, with the three interacting levels arranged in a cascade configuration, see Fig. 1]. In addition to the large and rapidly changing index of refraction predicted by the theory, our experiment shows that, because of the two-photon nature of the effect, it is possible to observe it in a Doppler-broadened medium with much lower laser powers than have been used previously, by making use of a Doppler-free configuration. In particular, we are able to use a cw laser diode for the coupling beam and to let the coupling Rabi frequency (i.e., the dynamic Stark shift of the upper level) be much smaller than the full Doppler width of the probe transition.

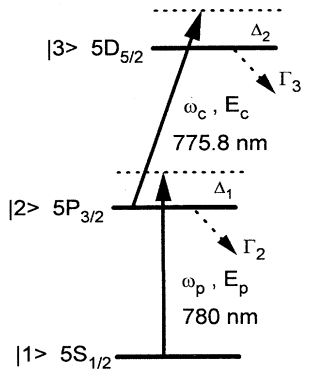

FIG. 1. Relevant energy levels of neutral rubidium atom.

In Fig. 1, the weak beam E_p at frequency ω_p probes the transition $|1\rangle \rightarrow |2\rangle$, while the levels $|2\rangle$ and $|3\rangle$ are coupled by the strong beam E_c at frequency ω_c. Under these conditions the reduced absorption has been explained as a combination of the ac-Stark splitting and quantum interference in the decay of the dressed states created by the coupling field [2,7]. In the bare-state picture, on the other hand, the EIT and the rapidly varying index of refraction can be thought of as being due to the coherence between the levels $|1\rangle$ and $|3\rangle$ which is induced by the probe and coupling fields [8]. When the atomic velocity distribution cannot be neglected, as is the case in our experiment, a straightforward semiclassical analysis [9] shows that the contribution of the atoms with velocity v to the complex susceptibility of the probe transition is given by

$$\chi(v)\,dv = \frac{4i\hbar g_1^2/\epsilon_0}{\gamma_{21} - i\Delta_1 - i\omega_p \dfrac{v}{c} + \dfrac{\Omega_c^2/4}{\gamma_{31} - i(\Delta_1 + \Delta_2) - i(\omega_p - \omega_c)\,v/c}}\,N(v)\,dv\,, \tag{1}$$

where the detunings Δ_1 (detuning of the probe laser from the transition $|1\rangle \rightarrow |2\rangle$) and Δ_2 (detuning of the coupling laser from the transition $|2\rangle \rightarrow |3\rangle$) are defined as the nominal detunings for an atom at rest, and the

 0031-9007/95/74(5)/666(4)$06.00

Doppler-free configuration (counterpropagating pump and probe beams) has been assumed. The decay rates $\gamma_{ij} = (\Gamma_i + \Gamma_j)/2$, where Γ_i is the natural linewidth of level $|i\rangle$ (we are neglecting collisional broadening; also note $\Gamma_1 = 0$, since $|1\rangle$ is the ground state). $2\hbar g_1$ is the dipole moment matrix element for the transition $|1\rangle \rightarrow |2\rangle$, $N(v)$ is the atomic velocity distribution (density of atoms with velocities between v and $v + dv$), and Ω_c is the Rabi frequency of the coupling beam. We note that for $v = 0$, the imaginary (absorptive) part of Eq. (1) immediately yields Eq. (1a) of the paper by Boller *et al.* [2].

The main approximation in the derivation of (1) is the neglecting of the population of levels $|2\rangle$ and $|3\rangle$, which is correct to first order in the weak probe beam amplitude E_p. The effect of the coupling beam, on the other hand, is included to all orders, and given by the term proportional to Ω_c^2 in the denominator. This term, which is responsible for the modification of the normal absorption-dispersion profile, arises in the bare-state formalism from a two-photon coherence induced between the levels $|1\rangle$ and $|3\rangle$, that is, a nonzero matrix element ρ_{13} to first order in E_p. Clearly, even for an atom at rest ($v = 0$), this term modifies the normal susceptibility in a nontrivial way which cannot be simply characterized either as a mere level shift or a broadening of the resonance. (Note in particular the important role played by the decay rate γ_{31}, which together with Ω_c^2 determines the size of the term under conditions of two-photon resonance, $\Delta_1 + \Delta_2 = 0$.) In fact, it is easily seen that when the middle level is very far detuned (Δ_1 larger than the Doppler width), this term yields the two-photon absorption profile from level $|1\rangle$ to level $|3\rangle$.

The two-photon nature of the Ω_c^2 term in (1) is evident from the fact that it depends on the sum of the two frequencies ω_c and ω_p (through $\Delta_1 + \Delta_2$). It is this fact that makes it possible to reduce substantially the effect of the atomic velocity distribution: If the two beams are counterpropagating, any given atom will see one upshifted and the other one downshifted, and, if ω_c and ω_p are sufficiently close, the root-mean square size of the resulting term, $(\omega_p - \omega_c)\, v/c$, can be much smaller than the full Doppler width. In our experiment, ω_c and ω_p are equal to about one part in 200; hence, we can see EIT with relatively low coupling beam power, even though the one-photon $|1\rangle \rightarrow |2\rangle$ transition is still fully Doppler broadened.

The experiment was done in a rubidium vapor cell. We measured the dispersion and the absorption of the probe beam simultaneously. As shown in Figure 1, the coupling laser of wavelength 775.8 nm couples the state $5P_{3/2}$ (state $|2\rangle$) to the state $5D_{5/2}$ (state $|3\rangle$), and the probe laser of wavelength 780.0 nm probes one hyperfine transition from the state $5S_{1/2}$ (state $|1\rangle$) to the state $5P_{3/2}$ (state $|2\rangle$), which is the Rb D_2 line. The experimental arrangement is shown in Fig. 2. The probe and coupling beams are orthogonally polarized and they popagate in opposite directions through a 76.0 mm long rubidium vapor cell kept at room temperature (20 °C). The natural linewidth Γ_2 of the rubidium D_2 line is about 6 MHz and the natural linewidth Γ_3 of the $5D_{5/2}$ state is about 0.97 MHz. The Doppler width of the D_2 line at room temperature is approximately 530 MHz.

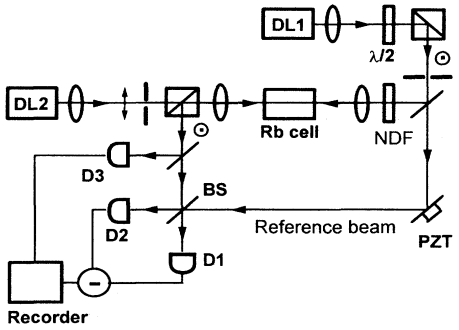

FIG. 2. Experimental arrangement. DL1 and DL2—diode lasers; BS—50/50 beam splitter; NDF—neutral density filter; and D1, D2, and D3—photodetectors.

A Mach-Zehnder interferometer for the probe beam is used to measure the dispersive properties of the atomic medium [10]. The small phase shift $\beta(\omega)L$ due to the atoms in the cell is detected using a homodyne arrangement [11]. The differential signal of the balanced homodyne detectors (D1 and D2) is given by

$$\Delta I_d(\omega) \propto 2|E_{\mathrm{LO}}|\,|E_s|\, e^{-\alpha(\omega)L/2} \cos[\phi_{\mathrm{LO}} + \beta(\omega)L], \quad (2)$$

where E_s is the signal field passing through the cell and E_{LO} is the local field through the other arm (reference beam). A neutral density filter ($T = 10^{-3}$) is used before the cell, so the signal beam is far below the saturation intensity of the D_2 transition and the condition $|E_s| \ll |E_{\mathrm{LO}}|$ is satisfied. $\alpha(\omega)$ is the absorption coefficient; $\beta(\omega)$ is the dispersion coefficient; L is the length of the rubidium cell; and ϕ_{LO} is the reference phase of the interferometer, which is reset to $\pi/2$ by a piezoelectric transducer for each frequency scan, so that $\Delta I_d(\omega) \propto \exp[-\alpha(\omega)L/2]\beta(\omega)L$ for $|\beta(\omega)|L \ll 1$. A static phase shift is introduced by the unbalanced lengths between the two arms of the interferometer. This phase shift is about 0.1 of a fringe over the 1.5 GHz range and is corrected in the dispersion curves. Each frequency scan of the probe laser takes 50 ms, during which time the interferometer has negligible drift. Both diode lasers are frequency and temperature stabilized to give a linewidth of about 5 MHz. The coupling laser (DL2) is a laser diode of wavelength 775.8 nm with maximum output power of 20 mW at the cell position. This coupling beam is focused by a 10 cm lens onto the cell. The coupling intensity at the beam waist is estimated to be 250 W/cm^2. The probe laser (DL1) is a laser diode of wavelength 780.0 nm. To get a good beam profile, a 0.5 mm aperture

is used. The probe beam is also focused by a 10 cm lens onto the cell to match the coupling beam. The local oscillator beam is about 1.0 mW in the reference arm and the signal beam is about 0.5 μW passing through the rubidium cell. The beam splitter (BS) for the homodyne detection is about 50/50. The detector D3 is used to measure the absorption coefficient $\alpha(\omega)$. A polarizer is used in front of it to eliminate the light scattered from the strong coupling beam by the windows of the cell.

When the coupling beam is blocked, typical absorption and dispersion curves of the probe transition are recorded, as shown in Figs. 3(a) and 3(b) (we concentrate only on one absorption line of Rb^{85} from $5S_{1/2}$, $F = 3$ to $5P_{3/2}$, $F' = 4$). The maximum absorption coefficient at the center frequency of the Doppler-broadened line is measured to be $\alpha \simeq 8.0 \times 10^{-2}$ cm^{-1}. When the coupling beam is applied and tuned to the resonance frequency ($\Delta_2 = 0$), a narrow dip at the center of the absorption profile appears [Fig. 3(c)]. The corresponding dispersion curve [Fig. 3(d)] is recorded simultaneously.

From Fig. 3(c) a new absorption coefficient $\alpha \simeq 3.8 \times 10^{-2}$ cm^{-1} is obtained at the center frequency. Using the dispersion curve in Fig. 3(d), we calculate the change in dispersion over frequency at the center frequency to be $d(\beta L)/d\nu|_{\nu_0} \simeq 19.4 \times 10^{-9}$ s, which yields the group velocity $v_g = c/13.2$, to be compared to the value $v_g = c/1.3$, when the coupling beam is blocked ($\Omega_c = 0$) and the probe is far from resonance ($\Delta_1 = -550$ MHz, where $d(\beta L)/d\nu$ has its maximum value in the absence of the coupling beam). This expected slowing down of the group velocity is the result of the rapid change in the refractive index due to the atomic coherence induced by the coupling beam.

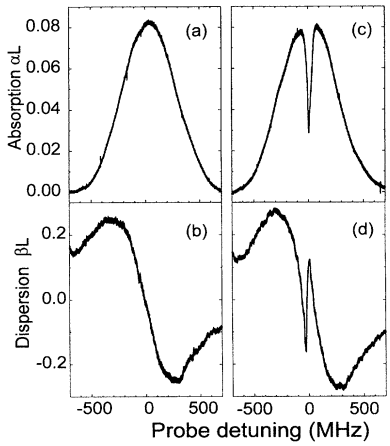

FIG. 3. Measured absorption αL and dispersion βL of the rubidium vapor cell vs probe detuning Δ_1. (a) Absorption with no pumping; (b) dispersion with no pumping; (c) absorption with pumping on resonance $\Delta_2 = 0$; and (d) dispersion with pumping on resonance $\Delta_2 = 0$.

If the Doppler broadening of the two-photon transition [i.e., the term in $\omega_p - \omega_c$ in Eq. (1)] is neglected altogether, and the velocity distribution $N(v)$ is conventionally taken to be Maxwellian, Eq. (1) can be integrated to yield the modified absorption and dispersion coefficients

$$\frac{\alpha(\omega)}{2} + i\beta(\omega) = \frac{2\sqrt{\pi}\hbar g_1^2 N_0 \omega_p}{\epsilon_0 u \omega_{12}} [e^{z^2}(1 - \mathrm{erf}z)], \quad (3)$$

with

$$z = \frac{c}{u\omega_{12}}\left(\gamma_{21} - i\Delta_1 + \frac{\Omega_c^2/4}{\gamma_{31} - i(\Delta_1 + \Delta_2)}\right), \quad (4)$$

(erf is the standard error function, u is the average thermal velocity of the atoms, and N_0 is the atomic density). The combination $e^{z^2}(1 - \mathrm{erf}z)$ appearing in Eq. (3) is the well-known plasma dispersion function (Voigt profile, convolution of a Gaussian with a Lorentzian) for a Doppler-broadened medium, but its argument is modified by the presence of the coupling beam, as shown by Eq. (4). We have plotted in Fig. 4 the absorption and dispersion profiles predicted by (3) and (4) for reasonable values of the parameters. The fact that the experimental curves have generally broader features than these theoretical plots is mostly due to the finite linewidth of the lasers used in the experiment. Note, in particular, that a large effect is predicted in this figure for Ω_c, as small as 40 MHz, well below the 530 MHz Doppler width of the one-photon ($|1\rangle \rightarrow |2\rangle$) transition. This is still the case when the small residual Doppler shift of the two-photon transition is fully taken into account, for the parameters of our experiment (the detailed theoretical treatment for this case will be the subject of a longer, forthcoming paper [9]).

In conclusion, we have reported the measurement of dispersive properties in an EIT medium, using cw lasers, and powers low enough that the ac-Stark shift caused by

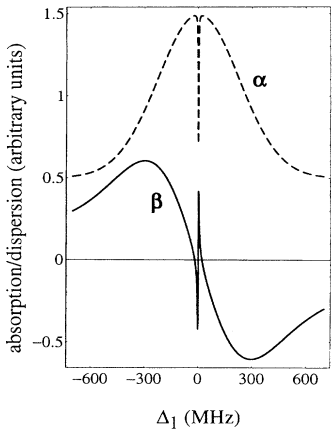

FIG. 4. Theoretical plots of normalized absorption α and dispersion β for $\Omega_c = 40$ MHz, $\Gamma_2 = 6$ MHz, $\Gamma_3 = 1$ MHz, $\Delta_2 = 0$, and Doppler width of 530 MHz. α curves are moved up by 0.5 unit for clearness.

the coupling beam is well below the full Dopler width of the probe transition. We have been able to achieve this new regime of operation by taking advantage of a Doppler-free configuration with nearly equal frequencies for the two one-photon transitions involved. Our experiment also demonstrates the usefulness of the homodyne detection technique for this type of measurement.

M. X. acknowledges support from the National Science Foundation through Grant No. PHY9221718.

[1] B. G. Levi, Phys. Today **45**, No. 5, 17 (1992); N. Singer, Science **258**, 32 (1992).

[2] J. E. Field, K. H. Hahn, and S. E. Harris, Phys. Rev. Lett. **67**, 3062 (1991); K.-J. Boller, A. Imamoğlu, and S. E. Harris, Phys. Rev. Lett. **66**, 2593 (1991).

[3] K. Hakuta, L Marmet, and B. P. Stoicheff, Phys. Rev. Lett. **66**, 596 (1991); G. Z. Zhang, K. Hakuta, and B. P. Stoicheff, Phys. Rev. Lett. **71**, 3099 (1993).

[4] S. E. Harris, J. E. Field, and A. Kasapi, Phys. Rev. A **46**, R29 (1992); S. E. Harris, J. E. Field, and A. Imamoğlu, Phys. Rev. Lett. **64**, 1107 (1990).

[5] S. P. Tewari and G. S. Agarwal, Phys. Rev. Lett. **56**, 1811 (1986).

[6] M. O. Scully, Phys. Rev. Lett. **67**, 1855 (1991); M. O. Scully and M. Fleischhauer, Phys. Rev. Lett. **69**, 1360 (1992); M. Fleischhauer *et al.,* Phys. Rev. A **46**, 1468 (1992); **49**, 1973 (1994).

[7] A. Imamoğlu and S. E. Harris, Opt. Lett. **14**, 1344 (1989); M. Fleischhauer *et al.,* Opt. Commun. **94**, 599 (1992).

[8] This second interpretation may be found, for instance, in the introductory paragraphs of the paper by Boller *et al.,* in Ref. [2].

[9] J. Gea-Banacloche, Y.-Q. Li, S.-Z. Jin, and M. Xiao, Phys. Rev. A **51**, 576 (1995).

[10] F. K. Kowalski, W. T. Hill, and A. L. Schawlow, Opt. Lett. **2**, 112 (1978); R. Schieder, Opt. Commun. **24**, 113 (1978).

[11] H. P. Yuen, Phys. Rev. A **13**, 2226 (1976).